

Computer Program for Control Rod Programming of BWR, Hiroshi Motoda, Takashi Kiguchi, Toshio Kawai

In the BWR in-core fuel management, one of the most important tasks is to determine the control rod programming that maximizes the cycle length under the various operational constraints. Recently, many papers¹⁻⁵ have been published on the optimal control rod programming; however, their core models are too simple for practical use. Using complete core model, a control rod program has to be generated by trial-and-error method, which consumes long computing time and much manpower.

We have developed a computer program which generates the suboptimal control rod program using the realistic three-dimensional simulator FLARE.⁶ To reduce the scale of the optimization problem, the problem was decomposed into two stages; i.e.,

1. Inner loop optimization: to determine the control rod positions, which minimize the mean square error of the power distribution from the target, at each burnup step
2. Outer loop optimization: to modify the target power distribution to minimize the residual control rods at the end of cycle.

The flow diagram of the program is illustrated in Fig. 1.

The inner loop optimization is formulated as

Control variable: rod positions R_i ($i = 1, \dots, I$)

Performance index:

$$J = \iiint [P(r) - P_{\text{target}}(r)]^2 dr \rightarrow \min \quad (1)$$

Constraints: criticality $k_{\text{eff}} = k_{\text{target}}$
 linear heat generation rate
 $LHGR(r) \leq MLHGR$
 critical heat flux ratio
 $CHFR(r) \geq MCHFR$
 stuck rod $R_i = R_i^{\text{fixed}}$.

The last constraint is used when some of rods are stuck or inserted for preventing fission product gas release.

The above nonlinear programming problem is solved by the method of approximate programming⁷; that is, the performance index and constraints are linearized with respect to the control rod movements to use linear programming repeatedly. To reduce the scale of the linear programming problem, the control rods are ganged into five- or ten-rod groups. The grouping is prepared for four patterns, and the patterns are changed periodically to assure local uniformity of burnup. Constraints for LHGR and CHFR are considered at about 100 nodes, which scatter properly in the core.

In the outer loop optimization, the "bottom peaked skewed Haling's power distribution"⁸ is used as the initial guess of the target distribution, and the target is revised as

$$P_{\text{target}}^{\text{New}}(r) = \left[1 + \alpha \frac{\Delta P(r)}{P(r)} \right] P_{\text{target}}^{\text{Old}}, \quad (2)$$

where $\Delta P(r)$ is the power increment, which compensates reactivity $\Delta k(r)$ of the control rod remaining at the end of cycle, and α is an input constant.

Test calculations are performed on the reference core shown in Table I. Table II lists a set of test results with skewing factor as a parameter. Cycle length is shown in the unit of Haling life for convenience.

A series of the rod pattern for case 1 is illustrated in Fig. 2. Insertion depth for each rod is given for a $\frac{1}{4}$ core using a conventional unit. Figure 3 shows the average fraction of inserted rod depth as well as the reactivity that the reactor would have if all rods were withdrawn. The rod density is stationary at the exposure of 2 GWd/T, owing to the poison curtain depletion characteristics. The core life is longer than that obtained by the Haling principle. As stated by Haling,⁸ the reactivity lifetime is extended at the expense of power peaking margin. The result clearly shows that the "deep and shallow principle" dominates; after a certain amount of exposure, all shallow rods are out and some of the deep rods turn to the shallow.

The maximum of FLPD in the core (MFLPD), behaves as shown in Fig. 4. They, of course, satisfy constraint as expected, and thermal margins are larger toward EOC contrary to our previous experience, which told us that there remained less margins as exposure proceeds. By the present method margins near EOC allow all rods withdrawn, because rods are not needed to maneuver power shapes. Rods can be withdrawn from the lower part of the core because this part has been depleted by the higher power density from the beginning, as seen in Fig. 5, and the depletion plays role of shallow rods.

References

1. W. B. TERNEY and H. FENECH, *Nucl. Sci. Eng.*, 39, 109 (1970).
2. H. MOTODA and T. KAWAI, *Nucl. Sci. Eng.*, 39, 114 (1970).
3. H. MOTODA, *Nucl. Sci. Eng.*, 46, 88 (1971).
4. A. SUZUKI and R. KIYOSE, *Nucl. Sci. Eng.*, 44, 121 (1971).
5. H. MOTODA, T. KAWAI, and T. KIGUCHI, *Trans. Am. Nucl. Soc.*, 15, 105 (1972).
6. D. E. DELP, D. L. FISHER, J. M. HARRIMAN, and M. J. STEDWELL, "FLARE: A Three-Dimensional Boiling Water Reactor Simulator," GEAP-4598, Gen-Electric Co. (1964).
7. R. E. GRIFFITH and R. A. STEWART, "A Nonlinear Programming Technique for the Optimization of Continuous Processing Systems," *Management Sci.*, 7, 379 (1961).
8. R. K. HALING, "Operating Strategy for Maintaining an Optimum Power Distribution Throughout Life," TID-7672 (1963).

TABLE I
Data of a Reference Core

Thermal output	1380 MW
Core flow rate	2.2×10^7 kg/h
Core inlet enthalpy	290 kcal/kg
Fuel bundle	
number of bundle	400
core lattice pitch	305 mm
active fuel length	3660 mm
fuel rod array	7 x 7
cladding o.d.	14.5 mm
fuel enrichment	2.1%
uranium in core	78.2 ton
Number of control rods	97
Number of poison curtains	172

TABLE II
Summary of Results of the Control Rod Program
Generated by the Present Method OPROD

OPROD				
Case No.	Skewing Factor	Cycle Length (Relative)	Min MCHFR	Max MFLPD
1	0.1	1.045	2.68	0.93
2	0.05	1.036	2.70	0.92
3	0	1.027	2.82	0.89
Haling Principle		1.000	3.37	0.74

Pattern change interval: 1.0 GWd/T.
Burnup calculation time step: 1.0 GWd/T.

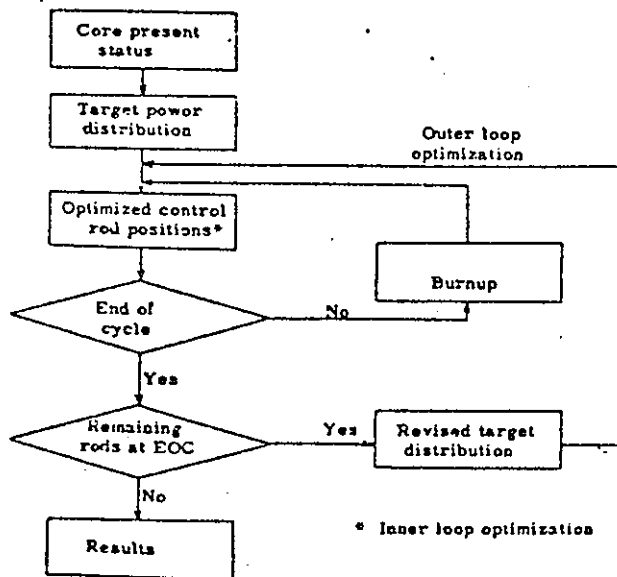


Fig. 1. Flow diagram of the program.

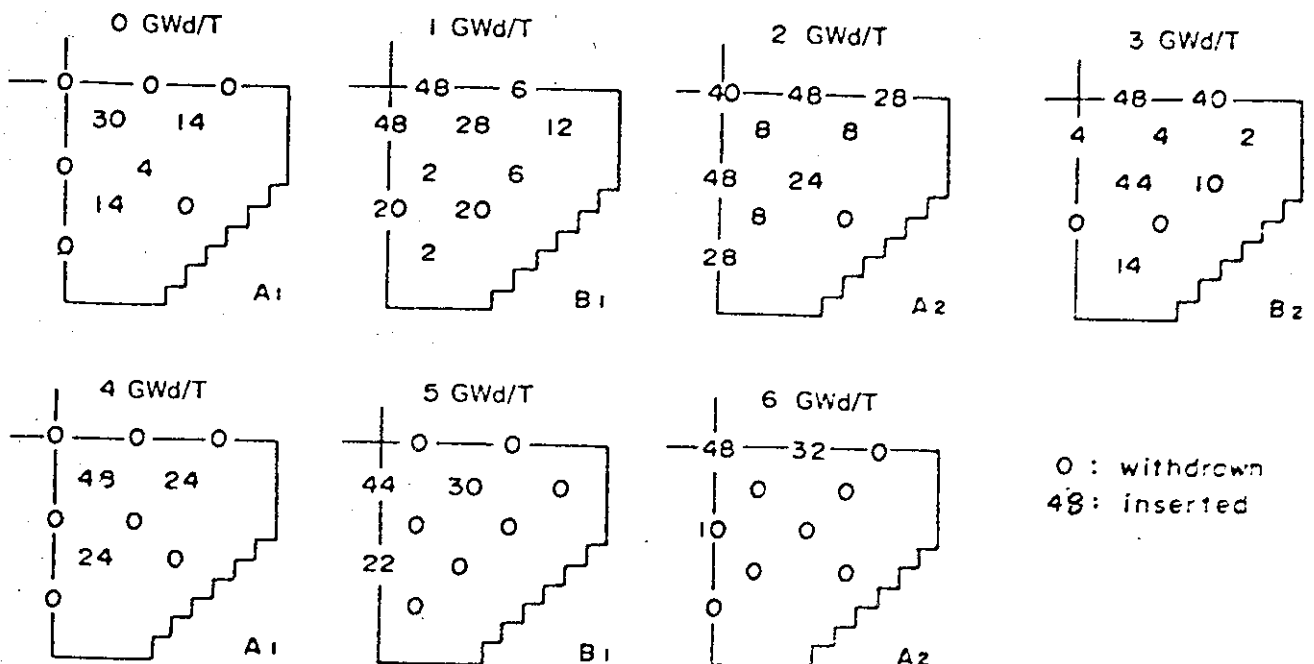


Fig. 2. Control rod program (case 1).

88090002

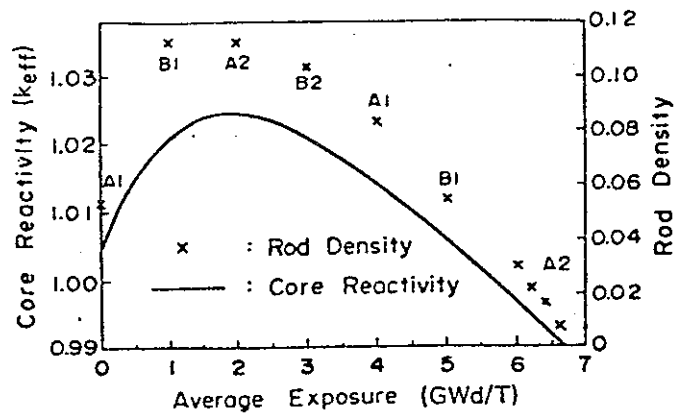


Fig. 3. Core reactivity (k_{eff} of core without control rods) and control rod density (case 1).

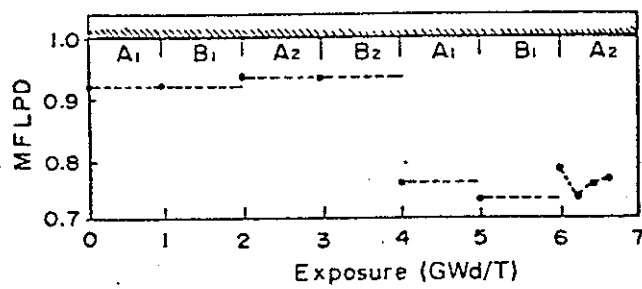


Fig. 4. Exposure versus maximum fraction of limiting power density as a result of control rod program by OPROD (case 1).

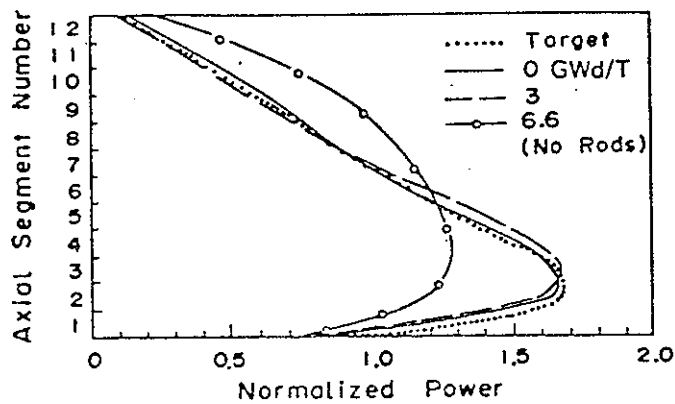


Fig. 5. Average axial power distribution versus exposure (case 1).